International Journal of Solids and Structures 000 (2018) 1–17

Contents lists available at ScienceDirect

International Journal of Solids and Structures

journal homepage: www.elsevier.com/locate/ijsolstr

Sand instability under constant shear drained stress path

M.J. Alipour, A. Lashkari*

Department of Civil and Environmental Engineering, Shiraz University of Technology, Shiraz, Iran

A R T I C L E I N F O

Article history:
Received 19 December 2017
Revised 3 May 2018
Available online xxx

Keywords:
Sand
Instability
Loss of uniqueness
Constitutive model
State

A B S T R A C T

Experimental findings have revealed that granular soils are vulnerable to pre-failure instability when subjected to constant shear drained (CSD) stress path. Using the concept of loss of uniqueness, it is shown that two dissimilar scenarios and accordingly, two independent criteria for granular soils in loose and dense states may lead to instability under CSD. The instability criteria are then applied in association with a state-dependent elastoplastic constitutive model taking into account possibility of elastic-plastic coupling. Numerical simulations have confirmed that instability in loose sands triggers prior to complete mobilization of the critical state stress ratio. However, instability of sands in dense state instigates at peak mobilized friction angle. A nearly unique linkage between stress ratio and state parameter at the onset of instability is predicted.

1. Introduction

Instability in soil mechanics is usually attributed to the rapidly growing generation of irrecoverable strains as caused by excessive external loads, or degradation of soil load carrying microstructure (e.g., Chu et al., 2003). Contemporary findings have confirmed that under some circumstances, granular soils are vulnerable to pre-failure instabilities. In other words, a soil may become unstable before its stress state fulfills Mohr-Coulomb or any soil failure criteria (e.g., Andrade, 2009; Andrade et al., 2013; Chu et al., 2015a; Chu et al., 2015b; Lashkari, 2016). Flow liquefaction under undrained (i.e., constant volume) condition, in which loose and very loose sands suffer from sudden progressive loss of shear strength beyond a transient peak shear strength is usually considered as a common type of pre-failure instability in sands. Experimental investigations and recent theoretical developments have indicated that flow liquefaction instability is triggered once loose soil reaches peak undrained shear strength where only about 70% of critical state friction angle may be mobilized (e.g., Sladen et al., 1985; Sun, 2013; Andrade et al., 2013; Lashkari et al., 2017). The vital importance of realistic evaluation of stability against flow slides in earth structures has motivated development of novel sand constitutive models in the recent years (e.g., Dafalias and Manzari, 2004; Kamai and Boulanger, 2012; Andrade et al., 2013; Sun, 2013; Lashkari, 2014, Lu and Huang, 2014; Zhao and Gao, 2015; Lashkari, 2016; Lashkari et al., 2017; Gao and Zhao, 2017; Xiao and Liu 2017; Lashkari and Yaghtin, 2018). On the other hand, numerous cases have been reported in the literature in which pre-failure instability occurs under drained condition (Chu et al., 2003, 2012, 2015a, 2015b; Sun, 2013; Dong et al., 2015). Eckersley (1990) reported experimental evidence supporting that slope failure begins under fully drained condition, and the observed rise in pore water pressure is an outcome of slope failure rather than the reason of it. In practice, an excessive increase in the mobilized effective stresses in soil mass corresponding to the applied external forces, may eventually lead to failure of slopes. However, increase in pore water pressure associated with the rise in water table, water infiltration and re-distribution of pore water pressure, precipitation, and irrigation may lead to the decrease in the effective stresses and consequently, soil shear strength drop (e.g., Brand, 1981; Harp et al., 1990; Dong et al., 2015). In the latter class of the slope failure problems [i.e., failures not associated with the increase in external loads], it has been suggested that the evolution of effective stress path in soil element can be idealized in the laboratory by the so-called constant shear drained (CSD) stress path in which the mean principal effective stress (or equally normal effective stress) decreases under fixed shear stress (e.g., Brand, 1981; Sasitharan et al., 1993; Skopek et al., 1994; Gajo et al., 2000; Sento et al., 2004; Chu et al., 2003, 2012, 2015a, 2015b; Azizi et al., 2009; Wanatowski et al., 2010; Dong et al., 2015). The mechanical behavior of loose sand subjected to CSD is schematically illustrated in Fig. 1. Following isotropic compression to state A, the sample is sheared along a conventional drained path (i.e., A→B) until the prescribed shear stress q_c is attained [*see* Fig. 1(a)]. Then, the sample is subjected to CSD (i.e., B→C→D) wherein the mean principal effective stress is reduced gradually under fixed shear stress (i.e., $q = q_c$). Typical curve for evolution of axial strain with falling mean principal ef-

* Corresponding author.
E-mail addresses: lashkari_ali@hamyar.net, lashkari@sutech.ac.ir (A. Lashkari).

https://doi.org/10.1016/j.ijsolstr.2018.06.003

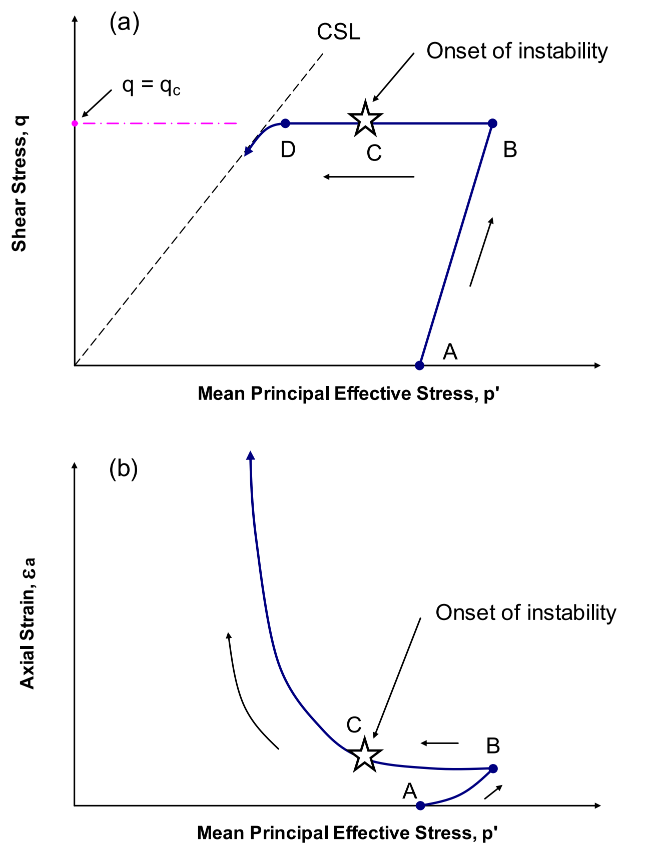

Fig. 1. Schematic description of loose sand behavior under CSD: (a) stress path, and (b) axial strain vs. mean principal effective stress.

fective stress [*see* Fig. 1(b)] indicates that the rate of irrecoverable axial strain generation becomes faster around C and thus, state C may be appointed as the onset of soil instability. Recently, Daouadji et al. (2010), Chu et al. (2012), and Dong et al. (2015) applied Hill's condition of stability [i.e., second-order work in Hill (1958)] to find a certain state for the onset of instability under CSD. Beyond D, the sample may exhibit severe limitation in following a constant shear stress path due to the lack of controllability (e.g., Nova, 1994; Chu et al., 2003; Daouadji et al., 2010). Sand unstable behavior under CSD has been experimentally and theoretically investigated by a number of researchers (e.g., Sasitharan et al., 1993; Skopek et al., 1994; Chu et al., 2003, 2012, 2015a, 2015b; Darve et al., 2004; Azizi et al., 2009; Wanatowski et al., 2010; Sun et al., 2013; Dong et al., 2015). Experimental studies have confirmed the similarities between collapse of loose sands under CSD and the catastrophic phenomena associated with the loose sands flow liquefaction instability (e.g., Sasitharan et al., 1993). While a majority of flow slide case histories have been reported for loose sand, some well-documented cases exist in the literature in which flow slide occurred in dense sand (*see* Chu et al., 2015a; Sento et al., 2004). Inspired by field observation, Fleming et al. (1989) suggested classifying flow slides into contractive and dilative categories.

Using the concept of loss of uniqueness, certain instability criteria for loose and dense sands subjected to CSD are obtained in this paper. The instability criteria are applied in conjunction with the state-dependent sand plasticity model of Lashkari et al. (2017). For four different sands, the constitutive model is calibrated against conventional drained and undrained data and then, its predictions are directly compared with data of CSD tests on the same sands. Finally, supplementary numerical simulations and discussions regarding the impact of initial condition and state variables on sand instability are presented.

2. General criteria for loss of stability under triaxial CSD

Loss of uniqueness, a concept based on the bifurcation theory, suggests that instability instigates once loss of equilibrium eventuates in multiple feasible solutions (e.g., Borja, 2002; Andrade et al., 2013; Mohammadnejad and Andrade, 2015). Under infinite small deformation rates, loss of uniqueness requires:

$$[[\dot{\sigma}']] : [[\dot{\varepsilon}]] = 0 \tag{1}$$

where $[[\dot{\varepsilon}]] = \tilde{\dot{\varepsilon}} - \dot{\varepsilon}$ is jump in strain rate due to duplicate solution for the velocity field [i.e., $(\tilde{\mathbf{v}}, \mathbf{v})$]. Similarly, $[[\dot{\sigma}']]$ is jump in effective stress rate tensor associated with $[[\dot{\varepsilon}]]$. In triaxial stress and strain spaces, Eq. (1) takes the form of (e.g., Andrade et al., 2013):

$$[[\dot{p}']]\,[[\dot{\varepsilon}_v]] + [[\dot{q}]]\,[[\dot{\varepsilon}_q]] = 0 \tag{2}$$

In Eq. (2), $p'\,[=(\sigma'_a + 2\sigma'_r)/3]$ is mean principal effective stress and $q\,[=(\sigma'_a - \sigma'_r)]$ is shear stress, where σ'_a and σ'_r are axial and radial effective stresses, respectively. $\varepsilon_v\,[=(\varepsilon_a + 2\varepsilon_r)]$ and $\varepsilon_q\,[=\frac{2}{3}(\varepsilon_a - \varepsilon_r)]$ are volumetric and shear strains, respectively, in which ε_a and ε_r are axial and radial strains. $[[\dot{q}]] = 0$ holds under CSD and thus, Eq. (2) reduces into:

$$[[\dot{p}']]\,[[\dot{\varepsilon}_v]] = 0 \tag{3}$$

Two possible independent solutions for Eq. (3) are $[[\dot{\varepsilon}_v]] = 0$ and $[[\dot{p}']] = 0$. The outcome and physical meaning behind each scenario is further discussed in the following sections.

2.1. General criterion for type I of stability where $[[\dot{\varepsilon}_v]] = 0$

Constitutive equations for elastoplastic models formulated in terms of triaxial stress and strain rate variables can be manipulated into straightforward matrix representations linking effective stress to total strain rates variables (e.g., Yang and Li, 2004; Andrade et al., 2013; Sun, 2013; Lu and Huang, 2014; Lashkari, 2016; Lashkari et al., 2017):

$$\begin{Bmatrix} \dot{p}' \\ \dot{q} \end{Bmatrix} = \begin{bmatrix} D_{pp} & D_{pq} \\ D_{qp} & D_{qq} \end{bmatrix} \begin{Bmatrix} \dot{\varepsilon}_v \\ \dot{\varepsilon}_q \end{Bmatrix} \tag{4}$$

where D_{pp}, D_{pq}, D_{qp}, and D_{qq} are components of the elastoplastic stiffness matrix $\left(\text{i.e., } \mathbf{D} = \begin{bmatrix} D_{pp} & D_{pq} \\ D_{qp} & D_{qq} \end{bmatrix}\right)$ which are uniquely related to the specific constitutive model under discussion. Since $\dot{q} = 0$ strictly holds under triaxial CSD, the calculated volumetric strain rate from Eq. (4) becomes:

$$\dot{\varepsilon}_v = \frac{1}{\det \mathbf{D}} D_{qq}\,\dot{p}' \quad if \quad \det \mathbf{D} \neq 0 \tag{5}$$

Considering Eq. (5), the first possible solution for Eq. (3) (i.e., $[[\dot{\varepsilon}_v]] = 0$) takes the form:

$$[[\dot{\varepsilon}_v]] = \frac{1}{\det \mathbf{D}} D_{qq} \left[[\dot{p}']\right] = 0 \quad if \quad \det \mathbf{D} \neq 0 \tag{6}$$

The only admissible solution for Eq. (6) is $D_{qq} = 0$ since in Section 2.2; it is mathematically shown that $[[\dot{p}']] = 0$ necessitates $\det \mathbf{D} = 0$, which is unacceptable here [*see* Eqs. (5) and (6)].

2.2. General criterion for type II of stability where $[[\dot{p}']] = 0$

Considering that $[[\dot{q}]] = 0$ always holds in triaxial CSD, Eq. (4) turns into a characteristic value problem in the following form when $[[\dot{p}']] = 0$: